



PERGAMON

Vision Research 41 (2001) 1321–1332

Vision  
Research

www.elsevier.com/locate/visres

# Visual areas and spatial summation in human visual cortex

William A. Press, Alyssa A. Brewer, Robert F. Dougherty, Alex R. Wade,  
Brian A. Wandell \*

*Psychology Department, Stanford University, Jordan Hall, Building 420, Stanford, CA 94305, USA*

Received 3 May 2000; received in revised form 19 February 2001

## Abstract

Functional MRI measurements can securely partition the human posterior occipital lobe into retinotopically organized visual areas (V1, V2 and V3) with experiments that last only 30 min. Methods for identifying functional areas in the dorsal and ventral aspect of the human occipital cortex, however, have not achieved this level of precision; in fact, different laboratories have produced inconsistent reports concerning the visual areas in dorsal and ventral occipital lobe. We report four findings concerning the visual representation in dorsal regions of occipital cortex. First, cortex near area V3A contains a central field representation that is distinct from the foveal representation at the confluence of areas V1, V2 and V3. Second, adjacent to V3A there is a second visual area, V3B, which represents both the upper and lower quadrants. The central representation in V3B appears to merge with that of V3A, much as the central representations of V1/2/3 come together on the lateral margin of the posterior pole. Third, there is yet another dorsal representation of the central visual field. This representation falls in area V7, which includes a representation of both the upper and lower quadrants of the visual field. Fourth, based on visual field and spatial summation measurements, it appears that the receptive field properties of neurons in area V7 differ from those in areas V3A and V3B. © 2001 Elsevier Science Ltd. All rights reserved.

*Keywords:* Functional MRI; Visual cortex; Cortical magnification; Spatial summation; Area V1, V3A, V3B, V7

## 1. Introduction

Using well-defined protocols and stimuli, the location of visual areas V1, V2 and V3 and the boundaries between them can be measured in an individual human subject during 30-min experiments. There is excellent agreement on experimental methods for partitioning occipital lobe into well-defined visual areas (DeYoe, Carman, Bandettini, Glickman, Wieser, Cox, Miller, & Neitz, 1996; Sereno, Dale, Reppas, Kwong, Belliveau, Brady, Rosen, & Tootell, 1995; Engel, Glover, & Wandell, 1997; Goebel, Khorram-Sefat, Muckli, Hacker, & Singer, 1998; Wandell, 1999). However, there are few reports that describe retinotopic and stimulus–response measurements in dorsal and ventral occipital cortex. Moreover, there are significant differences in the exist-

ing reports (Smith, Greenlee, Singh, Kraemer, & Hennig, 1998; Tootell et al., 1997; Wandell, 1999). In this paper we describe new fMRI measurements of the retinotopic organization and stimulus–response properties within human dorsal occipital cortex.

We find that the retinotopic maps on dorsal cortex have several distinct central representations: the foveal representation within V1/2/3 spreads onto the dorsal surface. A second representation falls at the confluence of areas V3A and V3B, while a third central representation is further anterior within area V7. The retinotopic maps of these central field representations suggest there are significant differences in the properties of the receptive fields of neurons within these cortical regions. To explore this hypothesis, we measured how the amplitude of the fMRI signal from the central representation depends on the spatial extent of the stimulus. These summation experiments support the hypothesis that the receptive fields of neurons in area V7 differ from those of neurons in V3A/B. In the Discussion we review hypotheses that might explain these differences.

\* Corresponding author. Fax: +1-650-7230993.

E-mail address: wandell@stanford.edu (B.A. Wandell).

## 2. Methods

### 2.1. Subjects

fMRI signals were measured in six (WAP, BAW, ARW, DR, BB, AH) right-handed males between the ages of 26 and 48. All experiments were undertaken with the understanding and written consent of each subject.

### 2.2. MRI methods

Anatomical MR images were obtained using a 1.5 T GE Signa scanner. Subjects were supine within the bore of the magnet and used a bite-bar to minimize head movements. Structural T1-weighted contrast images (TE = minimum full, TR = 33 ms, FA = 40 deg, spatial resolution =  $0.9 \times 0.9 \times 1.2 \text{ mm}^3$ ) were acquired with a GE volume head coil. These measurements provided a basic coordinate frame for representing all of the functional data.

Functional T2\*-weighted BOLD contrast images were acquired using a gradient-echo spiral k-space sequence (Glover & Lai, 1998; Kwong et al., 1992; Meyer, Hsu, Nishimura, & Macovski, 1992; Ogawa et al., 1992) in both a 1.5 T GE scanner and a 3T GE scanner. In the 1.5 T scanner, the receiving coil was a custom-built semi-cylindrical cradle surface coil; functional data were acquired in 16 planes using one spiral scan (TE = 40 ms, TR = 2000 ms, FA = 90°, inplane resolution =  $3.1 \times 3.1 \text{ mm}^2$ ) or 12 planes using two interleaved spiral scans (TE = 40 ms, TR = 1500 ms, FA = 90°, inplane resolution =  $2.7 \times 2.7 \text{ mm}^2$ ). In the 3 T scanner, the receiving coil was a custom-built close-fitting head coil; functional data were acquired in 16 planes using two spiral scans (TE = 30 ms, TR = 1000 ms, FA = 61°, inplane resolution =  $2 \times 2 \text{ mm}^2$ ). For all functional scans, plane thickness was 4 mm and plane orientation was either coronal or orthogonal to the calcarine fissure.

### 2.3. Data analysis

Briefly, the anatomical data were used to identify the locations of the cortical gray matter (Teo, Sapiro, & Wandell, 1997). Using custom software, the functional MRI measurements from each session were registered to the high-resolution anatomical scan of the subject's brain. To improve sensitivity, only data from gray matter voxels were analyzed for activity. Linear trends were removed from the fMRI time series and activity was measured by correlating the time series with a harmonic at the stimulus alternation frequency (1/36) Hz.

The data were then displayed on a three-dimensional representation of the boundary between white and gray

matter, or on a flattened representation of this same boundary. These surface renderings were computed using methods described elsewhere (Wandell, Chial, & Backus, 2000) that are distributed on the Internet [<http://white.stanford.edu>].

Cortical magnification maps were measured by identifying cortical paths falling near iso-angular representations in the flat map. These paths were converted to corresponding paths along the surface between the white and gray matter in the brain, and distances were measured along these three-dimensional paths using the methods described in Wandell et al. (2000). The full process comprises many steps, and these steps along with the source code will be described in a separate manuscript (Wandell, Brewer, Press, & Logothetis, 2001).

### 2.4. Stimuli

In the 1.5 T system, stimuli were presented on a flat-panel LCD (NEC 2000) contained within a shielded box present in the magnet room. The box was 4.3 m from the subject. Subjects viewed the flat-panel LCD through a set of binoculars with approximately eight-fold magnification, yielding an effective viewing distance of about 0.54 m. The display, calibrated using a PhotoResearch Spectroradiometer, had a mean luminance of 30 cpd/m<sup>2</sup> and all stimuli were shown at maximum contrast, ~90%. A fixation point was present at all times. In the 3 T system, stimuli were projected from a Sanyo LCD projector onto a screen mounted within the bore of the magnet. The mean luminance was 20 cpd/m<sup>2</sup>. The retinotopy experiments were performed using both systems. The spatial summation experiments were performed using the 3 T system.

Retinotopic organization with respect to the angular dimension was measured using a rotating wedge (width = 90° angle). Retinotopic organization with respect to eccentricity was measured using a thin expanding ring (width = 1/8 of the maximum stimulus radius). When measured in the 1.5T (3T) system the maximum stimulus radius subtended 16° (20°) visual angle. These stimuli produce a traveling wave of activity in retinotopically-organized areas, and the phase of activity at a given location in cortex uniquely identifies the location in space it represents (Engel et al., 1997; Engel et al., 1994). Both stimuli had a dartboard structure (radial spatial frequency = 1 cpd, angular frequency = 12 cyc/2p, flicker rate 4 Hz). The wedges and rings passed through a full display cycle over 36 s, and six cycles were shown in each experimental scan. We identified boundaries between areas by manually tracing reversals in response phase to the rotating wedge stimuli (Wandell, 1999).

Spatial summation measurements were performed in three subjects. Subjects fixated a central target and viewed either a solid circle that flickered at 4 Hz, or a circular dartboard that flickered at 4 Hz. The radius of the circular targets was varied across scans. The wedges of the dartboard spanned 15 deg of angle and each ring of the dartboard spanned 0.5 deg of visual angle.

The block design used a 36-s period in which the stimulus alternated with a constant background every 18 s. The responses (modulation percentage) were computed using the methods described in Wandell et al. (1999).

### 3. Eccentricity maps

Fig. 1a shows a three-dimensional rendering of the dorsal occipital lobe, extending partially into parietal cortex. The surface represents the boundary between white and gray matter that was identified by careful segmentation. Within this portion of the brain, each cortical region responds mainly to a visual stimulus at one retinotopic location. The colored overlay indicates the eccentricity (distance from the fovea) that causes a signal at that location. This eccentricity map was measured using a phase-encoding expanding ring stimulus

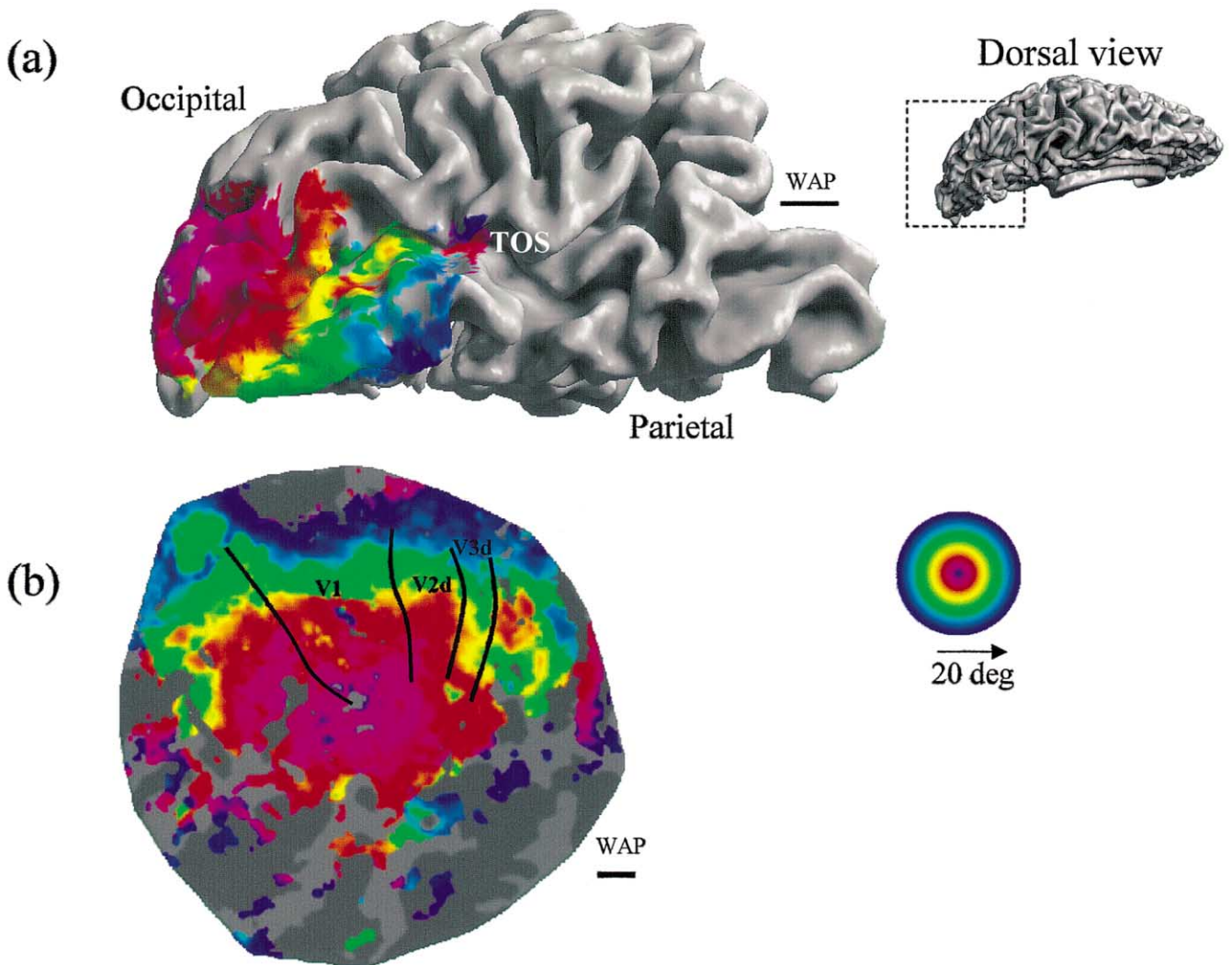


Fig. 1. Multiple distinct central representations in the dorsal occipital cortex. (a) The three-dimensional rendering of left dorsal occipital cortex (axial view; see inset at right) shows one large central representation at the confluence of areas V1, V2 and V3 near the occipital pole and extending laterally around the pole. Two other central representations are present in anterior dorsal occipital cortex. These representations fall near or within the transverse occipital sulcus (TOS). (b) A flat map shows the distinct central representations and other activity within the occipital lobe. The solid lines represent boundaries between the dorsal visual areas that were determined using data in Fig. 3. The colored inset shows the relation between color and visual field eccentricity. Scale bars are 1 cm.

(fovea to 20 deg; see inset) that is commonly used (Wandell, 1999). The data in this figure represent the average of five separate scans. To emphasize the dorsal activation, the overlay is shown only for measurements that are located near the transverse occipital sulcus (TOS) and correlated with the stimulus at a level of at least 0.35.

The eccentricity map contains three distinct central field representations. The largest of these falls in posterior occipital cortex at the confluence of areas V1, V2 and V3. A second distinct central field representation is visible at the fundus of the transverse occipital sulcus (TOS) where areas V3A and V3B are observed (Smith et al., 1998; Tootell et al., 1997). We have confirmed that a portion of this specific representation is within V3A by using angular retinotopic measurements (described in subsequent figures). This subject has a particularly clear third central field representation at a yet more anterior position in the TOS. Again, based on measurements of angular retinotopic organization, we have found that this third central representation falls within area V7 (Tootell et al., 1998).

Fig. 1b shows a flat map of these eccentricity measurements. The flattened representation includes all of the measurements from these scans, not just those along the TOS. Lines separate the dorsal boundaries between areas V1, V2 and V3. Just beyond these areas is the portion of flat map corresponding to the color overlay in the three-dimensional rendering. The boundaries between the areas were drawn using the angular retinotopic measurements shown below (Fig. 3).

Fig. 2 shows a three-dimensional rendering of the dorsal occipital lobe in a second subject. While there are significant differences in the shape of the TOS, three distinct central field representations are again visible and the general organization of the eccentricity map for the two subjects is the same. For this subject the central representation corresponding to V3A/B falls on the adjacent gyrus rather than within the TOS. Fig. 2b shows the corresponding flat maps from this subject and a flat map from a third subject.

The signals within the central representation of V3A/B differ from those in the two other central representations. Specifically, the central representation in V1/2/3 and the central representation in V7 include signals that correspond to the central 1–2 deg of the visual field (blue–magenta). However, the central representation near V3A/B contains signals beginning at 3–4 deg (red–orange). We confirm and analyze this difference quantitatively in several subsequent figures and additional experiments. In the Discussion, we offer several receptive field models for neurons in V3A/B and V7 that might explain these observations.

These functional maps contain imperfections. For example, consider the flattened representation of subject BAW in Fig. 2b. The middle of the green band contains

a small and surprising insertion of blue and red colors, indicating unexpected visual field locations. We make every effort to track down the source of these signals, and in this case we found that the unusual color corresponds to a spatial distortion that can be seen in the anatomical data, probably caused by a large blood vessel. These imperfections are present in fMRI data, and they are particularly salient in the study of individual, high-resolution, cortical maps that contain an expected representation. Even when we know the source to be a measurement artifact, we include these imperfections in the figures so that the reader can appreciate the limitations of the method.

#### 4. Visual areas

We identified the locations of several visual areas by measuring angular visual field representations (DeYoe et al., 1996; Engel et al., 1997; Sereno et al., 1995). Fig. 3a shows the angular visual field representations on a flat map that spans most of the occipital lobe. The color at each location represents the angle of the rotating wedge that caused an fMRI response (see the inset). Fig. 3a shows two reversals of the angular representation beyond dorsal V3, corresponding to two visual areas. Both areas include both an upper and lower visual field representation.

Fig. 3b shows an expanded view of flat maps from three subjects. These flat maps are centered near the central representation of V3A/B. In all three maps, the responses in V3A/B and V7 span upper and lower visual field quadrants.

The data in Figs. 1–3 are combined from three or more separate scans for each subject. In general, more averaging is required to identify the dorsal area boundaries than those between V1 and V2, which can be found in nearly every subject and every scan. The difference in our ability to mark the boundaries probably includes factors such as the large size of V1, differences in the cortical folding at the boundary of V1/V2, and the relatively short distance from V1/V2 to the RF coil. We have observed distinct representations for the two anterior representations in at least one hemisphere of the six subjects used for this study and bilaterally for the three subjects described in detail in this paper. However, unlike measurements of V1/V2, the dorsal images are not clearly identifiable in all subjects. At present, when we don't find all of these representations in one hemisphere or another, we attribute its absence to method limitations, not as an observation about that individual's visual cortex.

The phase reversal of the angular maps provides one important source of evidence to locate the boundary between two visual areas. A more general principle for retinotopic segregation of visual areas is this: two pieces

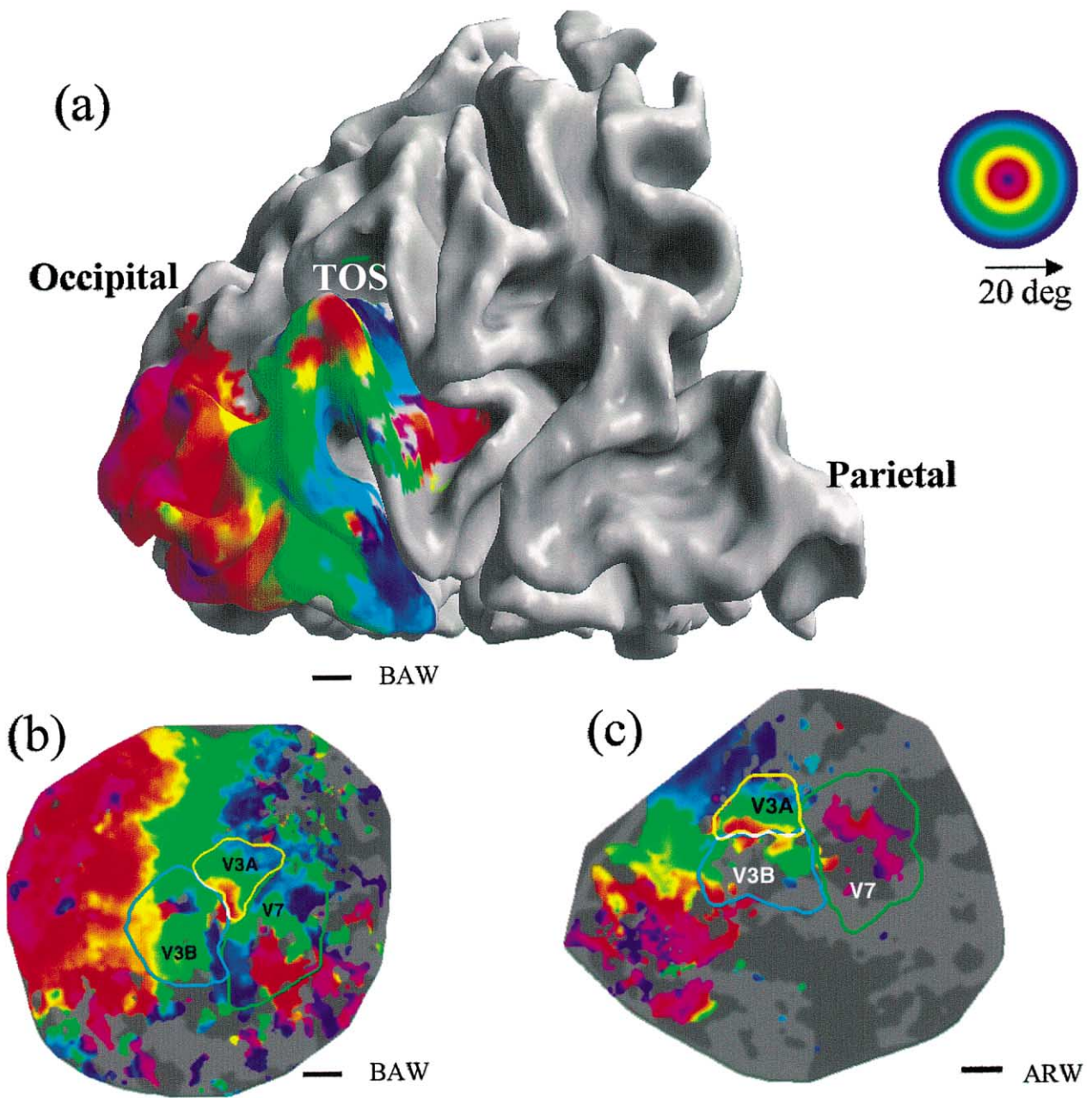


Fig. 2. Multiple distinct central representations in dorsal occipital lobe in two more subjects. (a) The three-dimensional rendering shows the eccentricity map near the TOS. In this subject (BAW) the central representation near V3A/B falls along the adjacent gyrus rather than the TOS. Flat eccentricity maps from subjects (b) BAW and (c) ARW. Other details as in Fig. 1.

of cortex that respond to the same portion of the visual field must belong to different visual areas. Considering the eccentric and angular maps together, it can be seen that cortex surrounding the central representation in V3A/B includes locations that represent the same portion of the visual field. This is a good reason to partition the region into at least two visual areas. Such a partition is generally consistent with the one suggested by Smith et al. (1998). Differing somewhat from their early report, we find that both the upper and lower quadrants are represented in V3B.

Although there is a third central field representation within area V7, we have not been able to measure a clear eccentric map within this area. Nonetheless, the distinct central representation can be seen clearly in all three subjects in Figs. 1 and 2, and we have verified its presence in many additional spatial-summation scans (see below). In these scans, the fMRI signals elicited by the 1.5 deg stimulus fell within a small region of V7 distinct from the central activation seen in V3A/B, and the cortical area that responded increased systematically with stimulus size.

## 5. Cortical magnification

In our subjects, the eccentric maps within V3A and V3B each span 2–3 cm. With an fMRI spatial sampling resolution of 2 mm, it is possible to measure the change in visual field eccentricity as a function of cortical position. Fig. 4 shows a measurement of this relationship for (a) area V3A and (b) area V3B.

The eccentricity map does not extend to visual field locations below 4 deg. This lower limit is visible from the colored overlays in Figs. 1 and 2; the central field representation in V3A/B does not include the same range of phases as those in V1/2/3 or V7.

The eccentricity map has the same functional form that describes cortical magnification in V1 and V2 (Engel et al., 1997). Within subject comparisons of the visual field maps in V1 and V3A/B suggest a compression of the V3A/B representation: Over the measured range (4–10 deg), there is roughly 30% less cortical area

per degree of visual angle in areas V3A/B than V1. The 2 mm sampling resolution, coupled with uncertainties in the segmentation and flattening process, do not permit a definitive measurement at this time.

The eccentricity map within area V7 (Figs. 1 and 2) is patchy and difficult to represent as a single function. In this regard, the data in V7 reflect an expanded foveal representation similar to the one measured in V1/2. It is evident from the flat maps in Figs. 1 and 2 that the fMRI signal in V7 includes phases that are similar to the central representation in V1/2/3 but differ from those in V3A/B.

## 6. Spatial summation

Next, we report measurements of spatial summation of the fMRI signal measured within areas V1/2/3 and near the central field representations in dorsal occipital

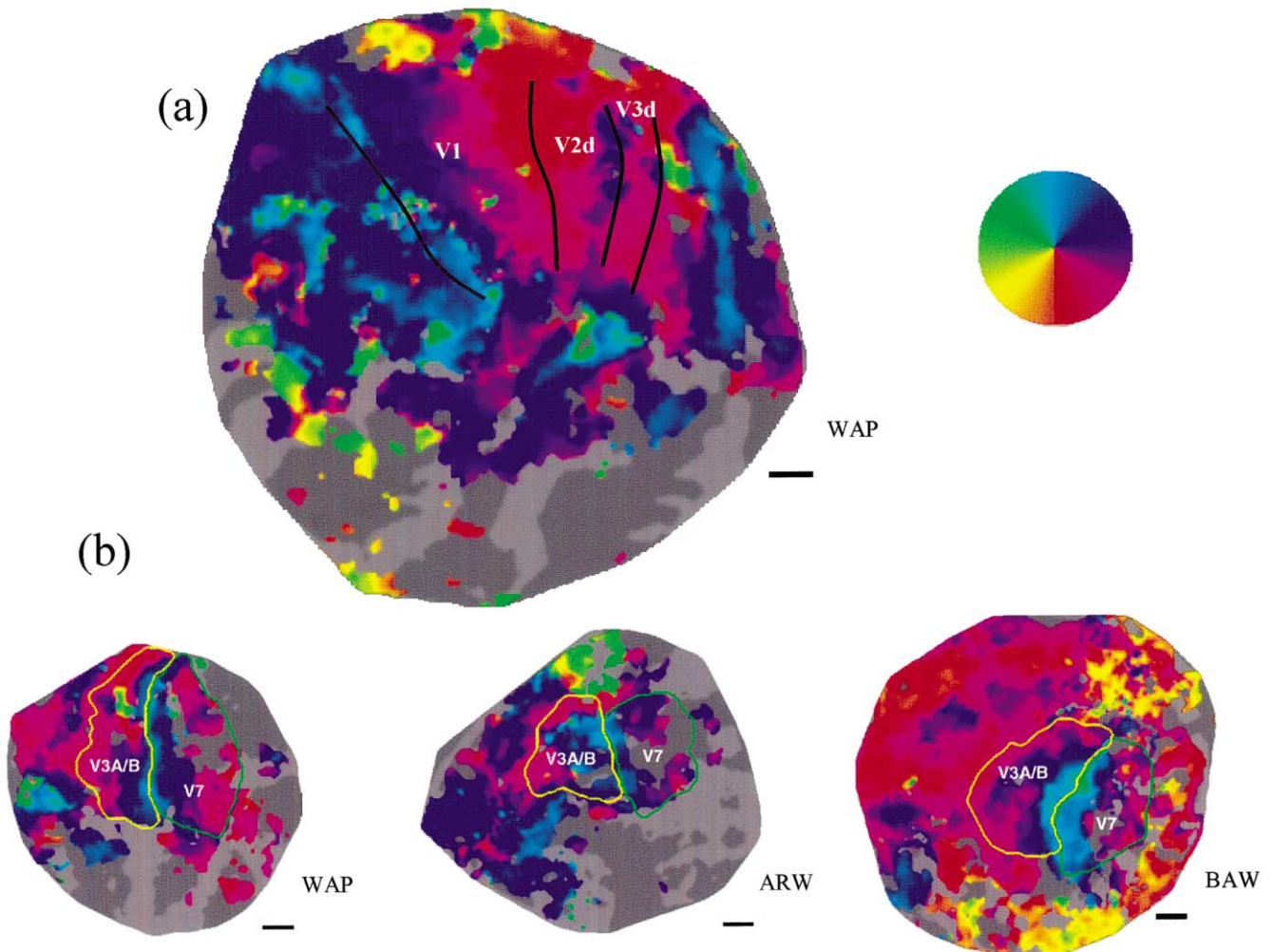


Fig. 3. Identification of visual areas using angular maps. (a) A flat map of WAP's occipital lobe is shown. The colors denote the angular representation at different positions (see inset). Lines are drawn at the reversals in the angular representation that define the boundaries between dorsal areas. (b) Smaller flat maps centered near the left hemisphere locations of V3A/B and V7 for three subjects. Other details as in Fig. 1.

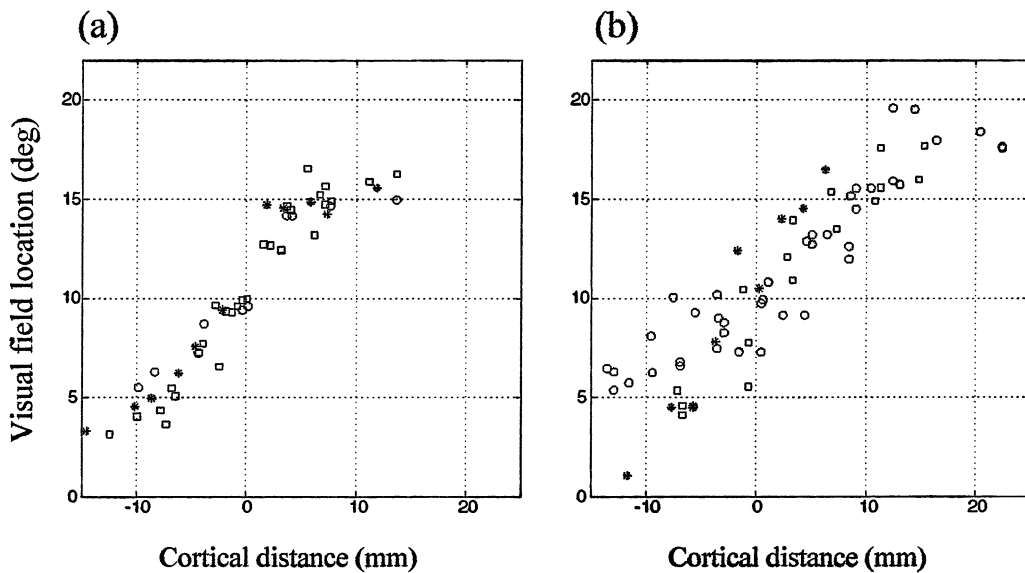


Fig. 4. Visual field eccentricity measured along the cortical surface. The horizontal axis measures distance along the cortical surface. The vertical axis measures eccentricity in the visual field. The data are aligned so that the representation at 10 deg eccentricity falls at 0 mm. Voxels whose response correlation was 0.20 or above were included for this analysis. All distances were measured along the three-dimensional surface that separates white and gray matter. Different symbols (o = WAP, \* = ARW, K = BAW) represent measurements from different subjects. The panels show measurements in (a) V3A and (b) V3B.

lobe. Specifically, we measured how the fMRI signal changes as the stimulus radius increases. We performed these measurements for two types of stimuli: a simple uniform disk and a dartboard target. In both cases, the measurements were obtained by selecting a region of interest (ROI) that responded to a small foveal target (1.5 deg radius). Then, in separate experiments, we measured the response within this ROI to targets of various sizes (1.5, 2, 2.5, 3, 6 deg radius).

Fig. 5 shows the fMRI response as a function of target size when measuring with a uniform disk. The responses in V1/2/3 show a similar pattern: The largest signal is obtained from a uniform disk whose size matches that of the disk used to select the ROI. As the disk radius increases, the magnitude of the fMRI signal decreases. The response asymptotes, so that even at the largest radius (6 deg), there is still some fMRI signal. For these visual areas, the edge of the uniform disk provides the strongest stimulus, and the effectiveness of the edge only spreads over a relatively narrow region. By the time the edge is 2 deg from the optimal position, the signal has become very small. Assuming that the response to a zero-radius disk (i.e. no disk) is zero, we have drawn smooth curves through the data that begin at the origin of the graph. The smooth curves were fitted assuming that summation is predicted by linear summation across a receptive field comprised of the difference of two Gaussians (Wandell, 1995, p. 144).

The data from V3A/B show a different pattern. The response magnitudes are roughly constant or even increase slightly as the disk radius grows. Hence, for these

areas either the photons from the disk itself constitute a signal or the edge can fall within a larger region and still evoke a powerful response. Given that the retina and early areas respond mainly to the edges rather than the level of photic stimulation, we think it is more likely that V3A/B responses are caused by edges too, but that these edges may fall within a larger summation region.

There are several significant differences between the summation measurements in V7 and the other two dorsal areas. In V3A/B disks with a radius larger than the 1.5 deg disk used to select the ROI produce greater signal than the original. The signal increases up to a disk radius of 2–3 deg. In area V7, however, the response never exceeds the measurement made using the 1.5 deg disk (as in V3A/B); nor does the response decline significantly (as in V1/2/3). This suggests that V7 spatial receptive fields differ, but the data in this study are inadequate to develop a quantitative model of the difference.

Fig. 6 shows the responses in these same visual areas when measuring with a black and white dartboard pattern. For this stimulus, unlike the uniform disk, the edge contrast within the central visual field remains constant as the disk radius increases. When measurements are made with these high contrast patterns, the fMRI responses within V1/2/3 ROIs remain constant as disk radius increases.

The responses in V3A/B increase with disk radius up to the measurement limit of 6 deg. This is consistent with the hypothesis that the neurons in these areas respond to contrast over larger regions of the visual

field than neurons in V1/2/3. The responses in V7 are similar to those in V1/2/3, not V3A/B: the responses are approximately equal for stimuli with a radius larger than 2 deg.

## 7. Discussion

### 7.1. The differences between V3A/B and V7

We have observed that the phase signals in the central representations of V3A/B differ from those in V1/2/3 and V7. How can we explain these differences? Fig. 7 illustrates one possible explanation for these differences based on the size and position of receptive fields in these areas.

Fig. 7a illustrates the relationship between the phase of the measured time series and the center of the receptive field. The figure shows an example of a relatively large receptive field (RF) located in the right visual field near the horizontal meridian. If the neuronal receptive fields within a visual area are large, symmetrical and restricted mainly to a hemifield, then the center of the receptive field will necessarily be shifted away from the fovea. For example, if receptive field sizes have a diameter no smaller than  $d$ , the center of a symmetric receptive field will be no closer to the fovea than  $d/2$ .

As a thin expanding ring stimulus travels through such a visual area, the fMRI time series will be similar to the one shown in the bottom part of the panel: The peak time series response (i.e. the response phase) mea-

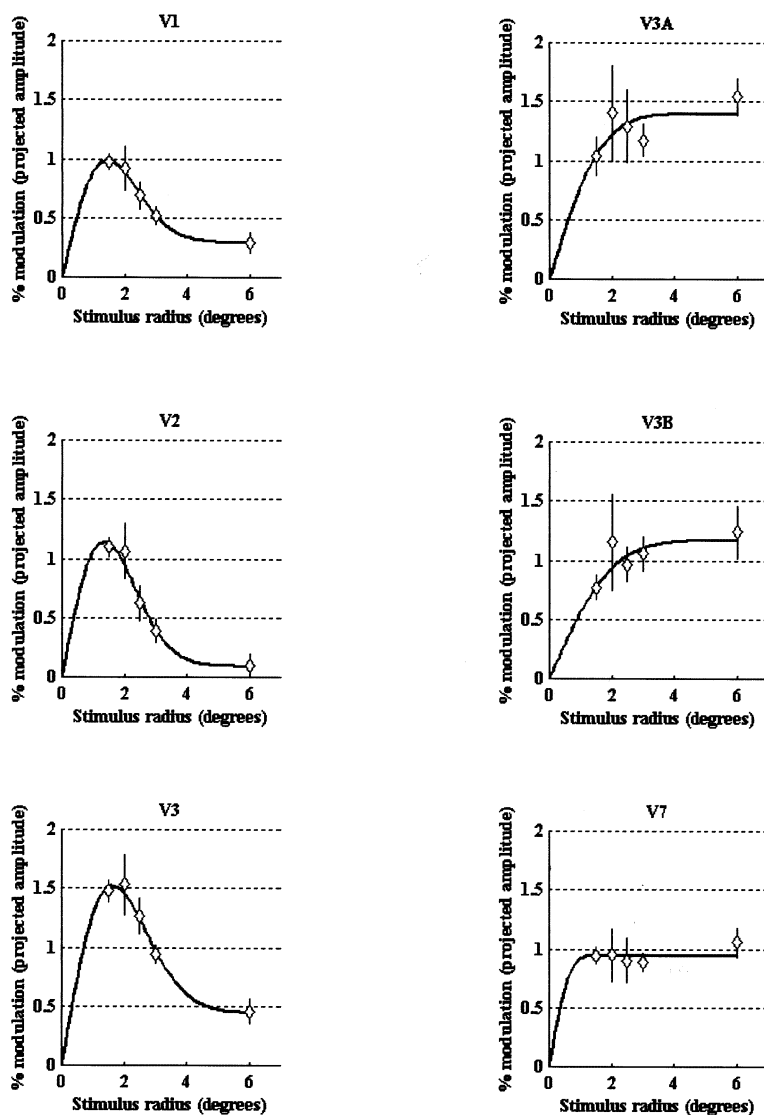


Fig. 5. Spatial summation measured with uniform disks. Within each area, voxels responding significantly to a small 1.5 deg target were chosen as the region of interest (ROI). Different panels show the fMRI response within these ROIs in various visual areas. The points are combined responses from subjects WAP and ARW. Error bars are 1 S.E.M.



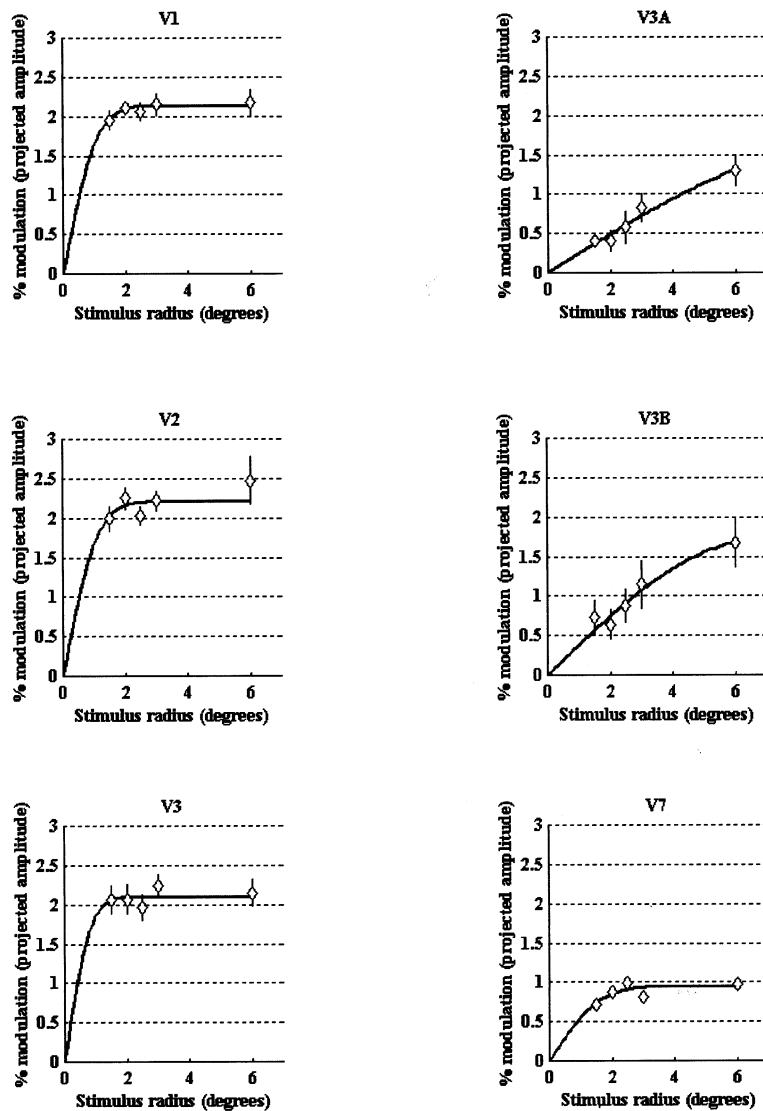


Fig. 6. Spatial summation measured using black and white dartboard contrast patterns. Other details as in Fig. 5.

sures the location of the receptive field center. In areas V3A/B, we can explain the absence of receptive field centers near the fovea by supposing these areas contain neurons with large receptive fields that do not extend significantly across the vertical midline. Conversely, in area V7 we can explain the presence of receptive field centers near the fovea by assuming that either the receptive fields are smaller (Fig. 7b) or they extend further across the midline (Fig. 7c).

Recall that the extent of spatial summation in V7 is smaller than that in V3A/B (Figs. 5 and 6). The receptive field arrangements in Fig. 7 could also explain the spatial summation differences between V7 and V3A/B. The spatial summation measurements are based on selecting an ROI using the responses to a small foveal disk. According to the hypothesis in Fig. 7b, this selected region would contain cells with smaller receptive fields than those in Fig. 7a. Hence, the spatial summa-

tion would be reduced because of the small RF size. Alternatively, suppose the receptive fields are the same size as V3A/B, but near foveal receptive fields span the vertical midline (Fig. 7c). In this case, the responsive neurons would include a large group whose position is centered on the vertical midline as well as a group centered in the right hemifield. Depending on the specific distribution of cell positions, the spatial summation for this ROI may well be smaller. Thus, differences in either the size (Fig. 7b) or the spatial distribution of the receptive fields (Fig. 7c) could explain the general differences in spatial summation between V3A/B and V7.

## 7.2. Related literature

How do the measurements reported here compare to published reports on retinotopic organization? Tootell

et al. (1997) reviewed the retinotopic organization of area V3A. They reported that in some instances V3A had a central representation distinct from the central representation of V1/2/3. However, they were uncertain whether this was a regular feature in most subjects; the issue is not specifically addressed in subsequent papers (e.g. Tootell et al., 1998; Tootell & Hadjikhani, 2001).

We measure a displaced central field representation for V3A/B in most subjects, apparently more often than Tootell and colleagues. Also, we have observed a difference between the signals within the V1/2/3 and V3A/B central representations. In their early measurements, Tootell and colleagues used an in-plane resolution of  $3.1 \times 3.1 \text{ mm}^2$  and the flat maps are usually blurred using a Gaussian kernel with 2.5 mm half-width. Over time the spatial resolution and sensitivity of fMRI have improved, so that our measurements are made at 2.1 mm and no spatial blurring is applied. The increased spatial resolution may make the displaced central representation and differences in eccentricity map values easier to detect.

Tootell et al. also showed that the fMRI response to a high-contrast thin ring pattern spreads across a larger distance in V3A than V1. The spatial summation measurements using the dartboard pattern (Fig. 5) confirm the larger summation in V3A/B. The spatial summation measurements using the uniform disk demonstrate further that the V1/2/3 responses are primarily due to the stimulus edge, so that the spread of activity is not due only to vascular blurring (Engel et al., 1997).

Smith et al. (1998) suggested that V3A be split into two areas, V3A and V3B. They argued from two observations. First, when measured with rotating wedge stimuli, they consistently observed a small silent zone within V3A that appeared to separate the activity into

two distinct cortical regions. Second, on one side of the silent zone (V3B) they could only measure a quadrant field representation, while the other side (V3A) contained a representation of both the upper and lower visual fields.

We support the subdivision proposed by Smith et al. Our support is based on our new angular and eccentricity maps and the principle that two regions of cortex that represent the same portion of visual space should be considered as parts of different visual areas (Figs. 1–3). While there is agreement in principle, there are two differences between our data and Smith's data. First, we find that V3B represents both the upper and lower quadrants. Second, using the expanding ring stimulus and spatial summation stimuli, we see activity in the zone they describe as silent. It is not uncommon, however, to measure a silent zone within a central representation during rotating wedge scan and then to find that this region represents the central fovea when using an expanding ring scan.

In a recent report, Tootell and Hadjikhani (2001) also describe a need to revise the map in dorsal occipital cortex (Tootell & Hadjikhani). They suggest an organization that includes V3B, but extends over a much larger region ( $10 \text{ cm}^2$ ) extending to MT+ on the lateral occipital cortex. Their measurements differ in some respects from those described here. First, they do not comment on the displaced central representation. Second, they report that visual field eccentricity in a region that appears to correspond to V3B is very unusual: There is significant foveal and peripheral activity but almost no parafoveal signal. In a graph of visual eccentricity as a function of cortical position (like Fig. 4 in this paper), they show measurements spanning 1 cm of cortex spaced at 0.25 mm. Such finely sampled

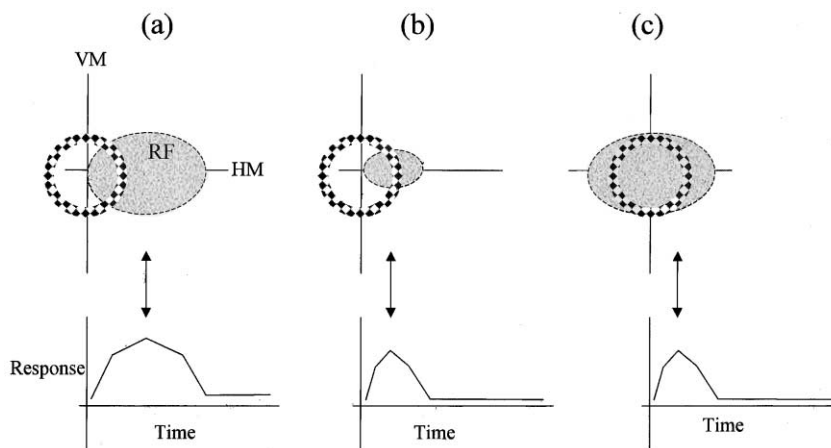


Fig. 7. Models of receptive field (RF) responses to a checkerboard expanding ring stimulus. (a) The top panel shows a large RF within the right hemifield. The patterned ring represents a stimulus traveling through the receptive field. The fMRI response to the ring stimulus is illustrated in the bottom panel. The arrow indicates the correspondence between the response phase and the RF center. There are two ways to shift the receptive field center closer to the vertical meridian (VM) and thus advance the phase of the time series. Either (b) shrinking the RF or (c) shifting its position to extend across the VM will move the RF center towards the VM (HM = horizontal meridian).

measurements are inconsistent with a spatial resolution of 3.1 mm (in-plane) followed by a 2.5mm Gaussian smoothing kernel. In all likelihood, these differences will be resolved in the future as more is published about the computational methods.

In a study on attention, Tootell et al. (1998) reported on the existence of a visual area, V7, just beyond V3A. In their initial report, they could only say confidently that this area represents at least a quadrant of the visual field. We confirm the existence of V7 and we show that it contains a representation of both the upper and lower visual fields as well as a distinct central representation (Figs. 1–3). The spatial summation within area V7 is surprisingly small, more like that in V1/2/3 than V3A/B.

Finally, we note that there have been other measurements of stimulus–response sensitivity in these dorsal regions. For example, Orban and his colleagues have suggested that this dorsal region contains a special representation for certain types of motion (Dupont et al., 1997; Van Oostende, Sunaert, Van Hecke, Marchal, & Orban, 1997). Braddick and colleagues also have analyzed motion selectivity in this region (Braddick, O'Brien, Wattam-Bell, Atkinson, & Turner, 2000). The relationship between these various types of stimulus selectivity and the retinotopic areas has not yet been determined.

## 8. Conclusion

Eccentricity maps on dorsal cortex include several distinct central representations, at the confluence of V1/2/3, the confluence of V3A/B and within V7. The signals in the central representation of V7 are similar to those in V1/2/3 and differ from those in V3A/B. The spatial summation measurements in V7 (Figs. 5 and 6) demonstrate this difference as well. The extent of spatial summation within V7 is similar to the V1/2/3 summation but different from V3A/B measurements. We offer two possible explanations of the summation measurements and retinotopic maps. According to one explanation the receptive field sizes of neurons in area V7 may be smaller than those in areas V3A/B; alternatively, the receptive fields near the fovea may extend further across the vertical midline in V7 than V3A/B.

## Acknowledgements

Supported by NEI EY30164, the Giannini Foundation, the Whitehall Foundation, and a McKnight Senior Fellowship.

## References

- Braddick, O. J., O'Brien, J. M., Wattam-Bell, J., Atkinson, J., & Turner, R. (2000). Form and motion coherence activate independent, but not dorsal/ventral segregated, networks in the human brain. *Current Biology*, *10*(12), 731–734.
- DeYoe, E. A., Carman, G. J., Bandettini, P., Glickman, S., Wieser, J., Cox, R., Miller, D., & Neitz, J. (1996). Mapping striate and extrastriate visual areas in human cerebral cortex. *Proceedings of the National Academy of Sciences of the USA*, *93*, 2382–2386.
- Dupont, P., De Bruyn, B., Vandenberghe, R., Rosier, A. M., Michiels, J., Marchal, G., Mortelmans, L., & Orban, G. A. (1997). The kinetic occipital region in human visual cortex. *Cerebral Cortex*, *7*(3), 283–292.
- Engel, S. A., Glover, G. H., & Wandell, B. A. (1997). Retinotopic organization in human visual cortex and the spatial precision of functional MRI. *Cerebral Cortex*, *7*(2), 181–192.
- Engel, S. A., Wandell, B. A., Rumelhart, D. E., Lee, A. T., Shadlen, M. S., Chichilnisky, E. J., & Glover, G. H. (1994). fMRI measurements in human early area V1: resolution and retinotopy. *Investigative Ophthalmology and Visual Science*, *35*, 1977.
- Glover, G. H., & Lai, S. (1998). Self-navigated spiral fMRI: interleaved versus single-shot. *Magnetic Resonance in Medicine*, *39*(3), 361–368.
- Goebel, R., Khorram-Sefat, D., Muckli, L., Hacker, H., & Singer, W. (1998). The constructive nature of vision: direct evidence from functional magnetic resonance imaging studies of apparent motion and motion imagery. *European Journal of Neuroscience*, *10*(5), 1563–1573.
- Kwong, K. K., Belliveau, J. W., Chesler, D. A., Goldberg, I. E., Weisskoff, R. M., Pncelet, B. P., Kennedy, D. N., Hoppel, B. E., Cohen, M. S., Turner, R., Cheng, H., Brady, T. J., & Rosen, B. R. (1992). Dynamic magnetic resonance imaging of human brain activity during primary sensory stimulation. *Proceedings of the National Academy of Sciences of the USA*, *89*, 5675–5679.
- Meyer, C. H., Hsu, B. S., Nishimura, D. G., & Macovski, A. (1992). Fast spiral coronary artery imaging. *Magnetic Resonance in Medicine*, *28*, 202–213.
- Ogawa, S., Tank, D., Menon, R., Ellermann, J., Kim, S., Merkle, H., & Ugurbil, K. (1992). Intrinsic signal changes accompanying sensory stimulation: functional brain mapping with magnetic resonance imaging. *Proceedings of the National Academy of Sciences of the USA*, *89*, 591–595.
- Sereno, M. I., Dale, A. M., Reppas, J. B., Kwong, K. K., Belliveau, J. W., Brady, T. J., Rosen, B. R., & Tootell, R. B. (1995). Borders of multiple human visual areas in humans revealed by functional MRI. *Science*, *268*, 889–893.
- Smith, A. T., Greenlee, M. W., Singh, K. D., Kraemer, F. M., & Hennig, J. (1998). The processing of first- and second-order motion in human visual cortex assessed by functional magnetic resonance imaging (fMRI). *Journal of Neuroscience*, *18*(10), 3816–3830.
- Teo, P. C., Sapiro, G., & Wandell, B. A. (1997). Creating connected representations of cortical gray matter for functional MRI visualization. *IEEE Transactions on Medical Imaging*, *16*(6), 852–863.
- Tootell, R. B., Hadjikhani, N., Hall, E. K., Marrett, S., Vanduffel, W., Vaughan, J. T., & Dale, A. M. (1998). The retinotopy of visual spatial attention. *Neuron*, *21*(6), 1409–1422.
- Tootell, R. B., Mendola, J. D., Hadjikhani, N. K., Ledden, P. J., Liu, A. K., Reppas, J. B., Sereno, M. I., & Dale, A. M. (1997). Functional analysis of V3A and related areas in human visual cortex. *Journal of Neuroscience*, *17*(18), 7060–7078.
- Tootell, R. B. H. & Hadjikhani, N. (2001). Where is 'dorsal V4' in human visual cortex? Retinotopic, topographic and functional evidence. *Cerebral Cortex*, in press.

- Van Oostende, S., Sunaert, S., Van Hecke, P., Marchal, G., & Orban, G. A. (1997). The kinetic occipital (KO) region in man: an fMRI study. *Cerebral Cortex*, *7*(7), 690–701.
- Wandell, B. A. (1995). *Foundations of Vision*. Sunderland, MA: Sinauer Press.
- Wandell, B. A. (1999). Computational neuroimaging of human visual cortex. *Annual Review of Neuroscience*, *22*, 145–173.
- Wandell, B. A., Brewer, A. A., Press, W. A., & Logothetis, N. (2001). FMRI measurements of retinotopic areas in macaque occipital lobe, in preparation.
- Wandell, B. A., Chial, S., & Backus, B. (2000). Visualization and measurement of the cortical surface. *Journal of Cognitive Neuroscience*, *12*(5), 739–752.
- Wandell, B. A., Poirson, A. B., Baseler, H., Boynton, G. M., Huk, A., Gandhi, S., & Sharpe, L. T. (1999). Color signals in human motion-selective cortex. *Neuron*, *24*(4), 901–909.